2023

Evaluating the impact of the hexosamine biosynthesis pathway and O-GlcNAcylation on glucose metabolism in bovine granulosa cells

Abigail M. Maucieri

David H. Townson

Molecular and Cellular Endocrinology 564 (2023) 111863

Contents lists available at ScienceDirect

Molecular and Cellular Endocrinology

journal homepage: www.elsevier.com/locate/mce

Evaluating the impact of the hexosamine biosynthesis pathway and O-GlcNAcylation on glucose metabolism in bovine granulosa cells

Abigail M. Maucieri [a], David H. Townson [a,b,*]

[a] Department of Animal and Veterinary Sciences, The University of Vermont, Burlington, VT, 05405, USA
[b] Department of Fisheries, Animal and Veterinary Sciences, The University of Rhode Island, Kingston, RI, 02881, USA

ARTICLE INFO

Handling Editor: Carolyn M. Klinge

Keywords:
Glucose
Glycolysis
Granulosa cell
Metabolism
O-GlcNAcylation
Ovary
Oxidative phosphorylation

ABSTRACT

Granulosa cells (GCs) of ovarian follicles prefer glucose as a metabolic substrate for growth and maturation. Disruption of glucose utilization via the hexosamine biosynthesis pathway (HBP) impairs O-linked N-acetylglucosaminylation (O-GlcNAcylation) and inhibits proliferation of bovine GCs of both small (3–5 mm) and large (>8.5 mm) antral follicles. Knowing that 2–5% of all glucose in cells is utilized via the HBP, the aim of this study was to characterize glucose metabolism in bovine GCs and determine the impact of the HBP and O-GlcNAcylation on metabolic activity. The GCs were initially cultured in serum-containing medium to confluency and then subcultured in serum-free medium in 96 well plates (n = 10 ovary pairs). The cells were exposed to vehicle and inhibitors of the HBP and O-GlcNAcylation for 24 h. Extracellular acidification rate (ECAR; an indicator of glycolysis) and oxygen consumption rate (OCR; an indicator of oxidative phosphorylation) of the GCs were measured using a Seahorse xFe96 Analyzer, including the implementation of glycolytic and mitochondrial stress tests. GCs from small antral follicles exhibited overall greater metabolic activity than GCs from large antral follicles as evidenced by increased ECAR and OCR. Inhibition of the HBP and O-GlcNAcylation had no effect on the metabolic activity of GCs from either type of follicle. The glycolytic stress test indicated that GCs from both types of follicles possessed additional glycolytic capacity; but again, inhibition of the HBP and O-GlcNAcylation did not affect this. Interestingly, inhibition of cellular respiration by 2-Deoxy-D-glucose impaired OCR only in GCs from small antral follicles, but exposure to the mitochondrial stress test had no effect. Conversely, in GCs from large antral follicles, oxidative metabolism was impaired by the mitochondrial stress test and was accompanied by a concomitant increase in glycolytic metabolism. Immunodetection of glycolytic enzymes revealed that phosphofructokinase expression is increased in GCs of small antral follicles compared to large follicles. Inhibition of O-GlcNAcylation impaired the expression of hexokinase only in GCs of small antral follicles. Inhibition of O-GlcNAcylation also impaired the expression of phosphofructokinase, pyruvate kinase and pyruvate dehydrogenase in GCs of both types of follicles, but had no effect on the expression of lactate dehydrogenase. The results indicate that GCs of small antral follicles possess greater aerobic glycolytic capacity than GCs from large antral follicles; but disruption of the HBP and O-GlcNAcylation has little to no impact on metabolic activity.

1. Introduction

Glucose is a major energy source for ovarian follicles, particularly the granulosa cells (GCs) (Armstrong et al., 1963; Boland et al., 1994; Boland et al., 1994a; Flint and Denton, 1969; Leroy et al., 2004a). Glycolytic metabolism is a major driver for follicles to successfully complete growth and steroidogenesis (Boland et al., 1993, 1994a). Although energy metabolism throughout the stages of folliculogenesis has not been well characterized, ovarian follicles can develop to pre-ovulatory size via glycolysis alone, regardless of oxygen availability (Boland et al., 1994). Conversely, depletion of glucose availability hinders the growth of follicles and impairs their ability to develop an antrum or to attain pre-ovulatory size (Boland et al., 1994). Thus, while the preferred energy substrate for metabolism within follicles is clearly glucose, the requirement for oxygen, and thus the importance of oxidative phosphorylation, during folliculogenesis is less certain. Recent studies suggest that GCs cultured under low (5%) vs. high (21%) oxygen conditions exhibit increased rates of glycolysis, proliferation, and phosphofructokinase activity with low levels of ATP, mitochondrial

* Corresponding author. 120 Flagg Rd, CBLS 289, Kingston, RI, 02881, USA.
E-mail address: dave_townson@uri.edu (D.H. Townson).

https://doi.org/10.1016/j.mce.2023.111863
Received 23 September 2022; Received in revised form 8 January 2023; Accepted 16 January 2023
Available online 21 January 2023

Abbreviations

ECAR	extracellular acidification rate
GCs	granulosa cells
HBP	hexosamine biosynthesis pathway
OCR	oxygen consumption rate
OGA	O-GlcNAcase
OGT	O-GlcNAc transferase

mass, mtDNA, and mitochondrial membrane potential (Shiratsuki et al., 2016). As the follicle is known to be a hypoxic environment (Van Blerkom et al., 1997), the previously mentioned study indicates granulosa cells are adapting to low oxygen conditions by a means of increased glycolysis (Shiratsuki et al., 2016).

Gonadotropin stimulation of antral follicles promotes glucose uptake, while simultaneously enhancing lactate production, suggestive of an upregulation of glycolytic metabolism (Allen et al., 1981; Boland et al., 1994; Boland et al., 1993; Flint and Denton, 1969; Hillier et al., 1985). Indeed, high concentrations of lactate within the follicular fluid of antral follicles is further indication that the follicle, and thus the GCs therein, preferentially metabolize glucose via glycolysis, rather than via oxidative phosphorylation (Leroy et al., 2004a; Nandi et al., 2007, 2008; Orsi et al., 2005). In sheep, for instance, glycolytic metabolism is the preferred pathway for gonadotropin induced differentiation of GCs (Campbell et al., 2010). Similarly in pigs, GCs of small antral follicles are very proliferative and have a high rate of proliferation that is accompanied by a metabolic shift toward aerobic glycolysis rather than oxidative phosphorylation (Costermans et al., 2019). This metabolic shift, sometimes referred to as the Warburg effect (Warburg, 1925), is common to cancer and other rapidly proliferating cell types (Sun et al., 2019; Tekade and Sun, 2017; Warburg, 1925). In the cow, small antral follicles (3–5 mm) contain GCs undergoing immense proliferation, and higher concentrations of lactate are detected in the follicular fluid than large antral follicles (>8.5 mm) in which GC proliferation has begun to wane (Maucieri and Townson, 2021). These observations suggest a metabolic shift occurs from glycolysis toward oxidative phosphorylation as follicles grow in the cow, and as the GCs therein shift from proliferation toward differentiation (i.e., luteinization), but these concepts have yet to be explored experimentally. Further evidence supporting the perception that GCs thrive initially in a glycolytic environment comes from the observation that glucose utilization by GCs of preantral follicles is stimulated by paracrine factors from oocytes, which favor glycolysis (Sugiura et al., 2005).

There are a variety of pathways in which GCs metabolize glucose. These include glycolysis, the pentose phosphate pathway, the polyol pathway, oxidative phosphorylation and the hexosamine biosynthesis pathway (HBP) (Kim et al., 2010). In the current study, the HBP is of interest because it accounts for 2–5% of glucose metabolism in all cell types, yet becomes an important conduit for glucose processing when glucose is in abundance and glycolytic metabolism predominates (Buse et al., 2002; Copeland et al., 2008; Ma and Hart, 2013). Glucose metabolized via the HBP forms uridine diphosphate N-acetylglucosamine (UDP-GlcNAc), a substrate which is then used to modify serine and threonine residues of proteins that might otherwise be phosphorylated (Hart and Akimoto, 2009). The addition of these sugar moieties is referred to as O-linked N-acetylglucosaminylation (O-GlcNAcylation), and is regulated solely by two enzymes, O-GlcNAc transferase (OGT) and O-GlcNAcase (OGA) (Bond and Hanover, 2015). The process of O-GlcNAcylation is highly dependent on nutrient availability and thus is proposed as a nutrient sensing mechanism within cells, regulating a vast array of cellular processes including proliferation, signal transduction, transcription, and metabolism. O-GlcNAcylation is implicated in a variety of disease states including cancer, neurodegenerative disease, and diabetes (Lefebvre et al., 2010; Ma and Hart, 2013; Wani et al., 2017). Dysregulation of O-GlcNAcylation is a hallmark of insulin resistance (Copeland et al., 2008). Coincidentally, insulin resistance is a common, transient occurrence in postpartum dairy cows that can, in part, result in delayed ovarian cyclicity (De Koster and Opsomer, 2013; Lucy, 2016a, 2016b). Additionally, the enzymes of the glycolytic pathway, including phosphofructokinase, aldolase, glyceraldehyde-3-phosphate dehydrogenase, enolase, pyruvate kinase, and lactate dehydrogenase all undergo O-GlcNAc modification (Dehennaut et al., 2008). Considering that O-GlcNAcylation alters the functionality of target proteins (Hardivillé and Hart, 2014), it is conceivable that glycolysis may be regulated by O-GlcNAcylation. In the cow, not only is the HBP active within ovarian follicles, but the degree of O-GlcNAcylation differs between small and large antral follicles (Maucieri and Townson, 2021), impacts GC proliferation (Maucieri and Townson, 2021; Wang et al., 2022) and impacts oocyte competence and fertilization (Zhou et al., 2019). An important connection between O-GlcNAcylation and glucose metabolism in GCs of developing antral follicles may exist in the cow as they relate to follicular growth and ovarian function.

Based upon the above observations, we have formulated the working hypothesis that the degree of O-GlcNAcylation in GCs of bovine ovarian follicles varies according to relative follicle size, and that manipulating O-GlcNAcylation influences the function and fate of bovine GCs. The objectives in the current study were to characterize the basal metabolism of GCs from small and large antral follicles, and to then evaluate the effects of manipulating the HBP (and, thus, O-GlcNAcylation) on GC metabolism. Assessing glucose metabolism in GCs of antral follicles is expected to provide insight about how follicles utilize energy for growth and maturation that can ultimately lead to ovulation.

2. Materials and methods

2.1. Isolation of granulosa cells

Bovine ovary pairs were collected from a slaughterhouse (Champlain Beef, Whitehall, NY) in 0.9% sterile saline with antibiotic-antimycotic (10,000 units/mL of penicillin, 10,000 μg/mL of streptomycin, and 25 μg/mL of Fungizone™; Gibco, Gaithersburg, MD). The ovaries were transported to the laboratory for processing at room temperature within 4–6 h of slaughter. Only ovaries morphologically staged to the mid-to-late estrous cycle were used (Ireland et al., 1980). Small (3–5 mm) and large (>8.5 mm) antral follicles were aspirated using a 21-gauge needle and luer lock syringe to collect granulosa cells (GCs). Samples were centrifuged at 84×*g* for 10 min at 4 °C to separate GCs from the follicular fluid. The pellet containing the GCs was separated from the follicular fluid and placed in cell culture as described below. The follicular fluid was discarded.

2.2. Granulosa cell culture

GCs were collected and cultured using a previously validated culture system (Maucieri and Townson, 2021). Briefly, the cells from individual ovary pairs were initially seeded into T25 flasks in DMEM/F12 medium (Gibco) containing 10% fetal bovine serum (Corning, Corning, NY) and antibiotic-antimycotic (10,000 units/mL of penicillin, 10,000 μg/mL of streptomycin, and 25 μg/mL of Fungizone™; Gibco) regardless of cell number/viability. The GCs were then incubated at 37 °C in 5% CO_2 and 95% air. After 72 h of culture (i.e., once the cultures had attained confluency), the GCs were switched to serum free conditions (described below) and were either treated for 24 h with the small molecule inhibitor of O-GlcNAcase (OGA), Thiamet-G (2.5 μM; Cayman Chemical, Ann Arbor, MI), or the inhibitor of O-GlcNAc transferase (OGT), OSMI-1 (50 μM; Cayman Chemical), for immunodetection of glycolytic enzymes (under altered conditions of O-GlcNAcylation), or trypsinized and sub-cultured for Seahorse analyses comparing GCs from small and large antral follicles using 96 well plates (as described below). In previous

work, GCs cultured under these conditions retain responsiveness to FSH and IGF-1 stimulation, express *STAR*, *FSHR*, and *CYP19A1* transcripts, secrete estradiol, and are sensitive to cytokine-induced cell death (Maucieri and Townson, 2021).

2.3. Immunodetection of glycolytic enzymes

Cultures of GCs exposed to the treatments (Control, Thiamet-G, or OSMI-1) for 24 h were washed with HBSS (Gibco) and trypsinized with 1 mL TrypLE (Gibco) to detach the cells from the T25 flasks. The resulting suspension of cells was quenched with an additional 5 mL DMEM/F12 + 10% FBS media, removed from flasks, and pelleted via centrifugation at 84×*g* for 5 min. Supernatants were removed, GC pellets were set on ice, and 500 μL RIPA lysis buffer was added for 10 min. GCs were further lysed by aspirating through a 27-gauge needle. The entire sample was vortexed for 15 s and centrifuged at 15,295×*g* for 10 min. The resulting pellet was discarded but the protein lysate (supernatant) was subjected to quantification using a bicinchoninic acid (BCA) colorimetric assay (Thermo Scientific). Absorbance was measured at 562 nm by a Synergy HT Plate Reader (BioTek, Winooski, VT). The samples were diluted in RIPA buffer and Lamelli sample buffer to standardize protein concentration prior to boiling at 100 °C for 1–3 min.

For electrophoresis, 10 μg of total protein was loaded into each well of a precast, stain free 10% gel (BioRad, Hercules, CA). Following protein separation, the gels were activated and imaged for quantification of total protein using the BioRad ChemiDoc Imaging System. The proteins were then transferred to PVDF membranes (BioRad) using a semi-dry transfer system for 1 h at 45 mA (Hoefer, Holliston, MA). Post transfer, the gels were reimaged using the ChemiDoc Imaging System to verify complete transfer of the separated proteins. Following transfer, the membranes were incubated in tris-buffered saline (TBS) solution with 5% BSA and 0.2% Tween20 (TBST; Fisher Bioreagents, Pittsburgh, PA) as blocking agents, and agitated using a platform rocker for 3 h at room temperature. Following the blocking step, the membranes were incubated overnight at 4 °C on a platform rocker with rabbit anti-hexokinase (1:2500, C64G5), phosphofructokinase (1:2500, D4B2), pyruvate kinase (1:2500, C103A3), pyruvate dehydrogenase (1:2500, C54G1) (Cell Signaling Technology, Danvers, MA), lactate dehydrogenase (1:2500, NBP1-48336) (Novus Biologicals, Littleton, CO), O-GlcNAc transferase (1:1000 D1D8Q) (Cell Signaling Technology), or O-GlcNAcase (1:1000, SAB00311) (Sigma) primary antibodies. Following incubation with the primary antibody, the membranes were washed with TBST under agitation in the following order: 2X for 10–30 s, 1X for 15-min, and 3X for 5-min before incubating in secondary antibody for 1 h at room temperature on a platform rocker. Goat-anti-rabbit and goat-anti-mouse antibodies conjugated to horse radish peroxidase (HRP) were used as the secondary antibodies (#7074, #7076 1:5000, Cell Signaling Technology). The membranes were washed as previously described and incubated in Clarity Western ECL Blotting Substrate (BioRad) for 5 min. Immunodetectable proteins were imaged on the ChemiDoc Imaging System. Protein values were standardized to total protein of the gel detected immediately after electrophoresis, prior to membrane transfer and immunodetection. Each protein of interest was quantified using Image J software (National Institute of Health).

2.4. Seahorse analyses

The GCs were sub-cultured to 96-well Seahorse XF microplates (Agilent Technologies, Santa Clara, CA) in serum-free DMEM/F12 medium containing a reduced concentration of ITS (insulin-10 ng/ml, transferrin-5.5 ng/ml, and sodium selenite-0.67 pg/ml) at a density of 75,000 cells/well. The GC cultures were exposed to 0.1% DMSO (Control), the HBP inhibitor, DON (6-diazo-5-oxo-L-norleucine, 50 μM; Cayman Chemical), the OGT inhibitor, OSMI-1 (50 μM, Cayman Chemical), or the OGA inhibitor, Thiamet-G (2.5 μM, Cayman Chemical), for 24 h. DON, OSMI-1, and Thiamet-G have all been previously validated as effective agents to disrupt global O-GlcNAcylation without adversely affecting the cells (Maucieri and Townson, 2021; Ortiz-Meoz et al., 2015; Walter et al., 2020; Yuzwa et al., 2008). The DMEM/F12 serum-free medium was exchanged with Seahorse XF DMEM medium (no glucose, glutamine, pyruvate, sodium bicarbonate, or phenol red, pH 7.5; Agilent Technologies) supplemented with 1 mM glucose. To prevent dilution of the treatments following the medium exchange, the treatments (DON, OSMI-1, Thiamet-G) were added again to the new medium at the appropriate concentration. The cultured GCs of small and large antral follicles were also subjected to glycolytic and mitochondrial stress tests as per the manufacturer's guidelines (Agilent Technologies). Briefly, these tests included three consecutive injections of treatments. For the glycolytic stress test, this entailed exposure of the cells to 10 mM glucose (glycolysis stimulant), followed by 1 μM Oligomycin (ATP synthase inhibitor), and then 50 mM 2-deoxy-glucose (an unmetabolizable form of glucose, used as a hexokinase and glycolysis inhibitor), separated by 18-min intervals. For the mitochondrial stress test, the cells were exposed to 1 μM Oligomycin (ATP synthase inhibitor), followed by 1 μM trifluoromethoxy carbonylcyanide phenylhydrazone (FCCP, uncoupling agent of the mitochondrial proton gradient), and then 0.5 μM Rotenone and Antimycin A(Complex I and III inhibitors), separated by 18-min intervals following an initial basal reading. Measured outputs were: extracellular acidification rate (ECAR) and oxygen consumption rate (OCR) in the conditioned culture medium and were acquired every 3 min automatically by the Wave software. Seahorse measurements of ECAR and OCR are direct measurements of the relative rates of aerobic glycolysis and oxidative phosphorylation, respectively (Zhang and Zhang, 2019). Measurements of ECAR and OCR were automatically generated by the Seahorse XFe96 Wave software. All the inhibitors used in the above-described experiments were sourced from Cayman Chemical.

2.5. Statistics

In the instance that a sample from an individual pair of ovaries was run in either duplicate or triplicate, the mean of the two or three wells corresponding to that ovary pair was used as the value in the corresponding statistical analyses. In all instances, the individual cow or "ovary pair" is considered the experimental unit. A paired *t*-test was used to compare enzyme expression between untreated GCs obtained from small and large antral follicles within the same ovary pair. A repeated measures one-way ANOVA followed by Dunnett's multiple comparisons was used to evaluate enzyme expression relative to treatment. A repeated measures two-way ANOVA followed by Bonferroni's multiple comparisons was used to evaluate Seahorse analyses relative to treatment and time, and within follicle size classifications. A paired *t*-test was used to evaluate OCR and ECAR at individual time points between GCs obtained from small and large antral follicles. Significant differences were declared at $P < 0.05$. Tests were performed using GraphPad Prism 8 statistical software.

3. Results

3.1. Granulosa cells of small antral follicles exhibit overall greater metabolic activity than those of large antral follicles

Overall, GCs cultured from small antral follicles exhibited overall greater metabolic activity than those from large follicles, as evidenced by greater ECAR (Fig. 1A, $P < 0.05$) and OCR (Fig. 1B, $P < 0.05$) under basal conditions.

3.2. Metabolic response to in vitro stress tests varies with antral follicle size

To evaluate further the metabolic capacity of the GCs from small and large antral follicles, cultured GCs were subjected to glycolytic and

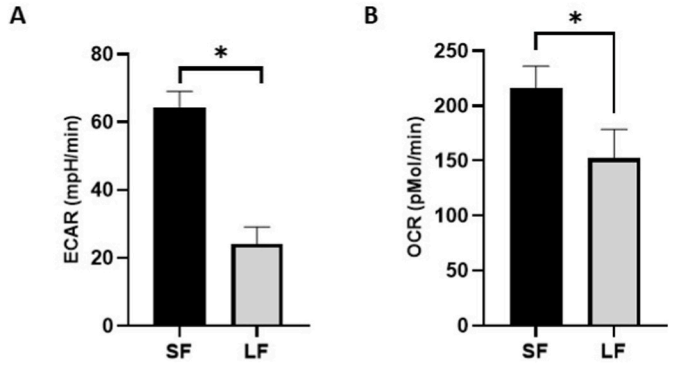

Fig. 1. Extracellular Acidification Rate (ECAR) and Oxygen Consumption Rate (OCR) of granulosa cells from bovine antral follicles according to follicle size. (**A**) ECAR (mpH/min) and (**B**) OCR (pMol/min) are depicted for small (SF; 3–5 mm) and large (LF; >8.5 mm) antral follicles. Results represent n = 10 ovary pairs, run in triplicate, with the mean±SEM of the respective measurement shown. Asterisks denote differences between SF and LF at $P < 0.05$.

mitochondrial stress tests. As seen in Fig. 2, the glycolytic stress test revealed that GCs from both small and large antral follicles respond favorably to excess glucose by increased ECAR (Fig. 2A; $P < 0.05$). Moreover, glycolysis (i.e., ECAR) remained elevated following inhibition of ATP Synthase via Oligomycin (Fig. 2C; $P < 0.05$), but there was no concomitant effect on oxidative phosphorylation (i.e., OCR) (Fig. 2D; $P > 0.05$). Inhibiting glycolysis with the glucose antagonist, 2-deoxy-D-glucose, decreased OCR in GCs from small antral follicles (Fig. 2F; $P < 0.05$), but had no effect on GCs from large antral follicles (Fig. 2F; $P > 0.05$) or on the ECAR of GCs from either follicle size (Fig. 2E; $P > 0.05$).

The mitochondrial stress test (Fig. 3) revealed that GCs only from large antral follicles were sensitive to manipulation of oxidative phosphorylation through electron transport, mitochondrial membrane, and/or ATP synthase mechanisms as evidenced by concomitant increases in ECAR and decreases in OCR. Specifically, oligomycin treatment, which prevents ATP synthase activity, increased ECAR (3A; $P < 0.05$) while simultaneously decreasing OCR (3B; $P < 0.05$). Uncoupling of the mitochondrial proton gradient via FCCP had no further effect on ECAR or OCR (3C and D, respectively; $P > 0.05$). However, inhibition of mitochondrial Complex I and III enzymes with rotenone and antimycin A, further increased ECAR (3E; $P < 0.05$), as it diminished OCR (3F; $P < 0.05$). There were no effects of these inhibitors on oxidative phosphorylation in GCs from small antral follicles (Fig. 3 A-F; $P > 0.05$).

3.3. Inhibition of the hexosamine biosynthesis pathway (HBP) and O-GlcNAcylation fails to impair granulosa cell metabolism, regardless of antral follicle size

Consistent with the above observations that overall metabolic activity is greater in GCs from small antral follicles compared to large antral follicles, evaluation of the effects of HBP manipulation revealed greater ECAR and OCR in GCs from small antral follicles compared to large antral follicles under control culture conditions (Fig. 4, compare open triangles vs. open circles, respectively; $P < 0.05$). Inhibition of the HBP via the GFAT inhibitor, DON (50 μM) had no effect on ECAR or OCR of GCs regardless of follicle size (Fig. 4A and B, $P > 0.05$). Similarly, inhibition of OGA (via Thiamet-G) and OGT (via OSMI-1) had no effect on the ECAR or OCR of GCs regardless of follicle size (Fig. 4C and D, $P > 0.05$). Additionally, and as expected (Maucieri and Townson, 2021), inhibition of the HBP decreased the expression of immunodetectable O-GlcNAcylated proteins in cultured GCs (results not shown).

3.4. Glycolytic enzyme expression varies by antral follicle size

As depicted in Fig. 5A and B, expression of immunodetectable phosphofructokinase was greater in GCs from small antral follicles compared to large antral follicles ($P < 0.05$). Expression of other key enzymes of glycolytic metabolism, including hexokinase, pyruvate kinase, pyruvate dehydrogenase, and lactate dehydrogenase, however, did not differ between the two antral follicle sizes (Fig. 5C; $P > 0.05$).

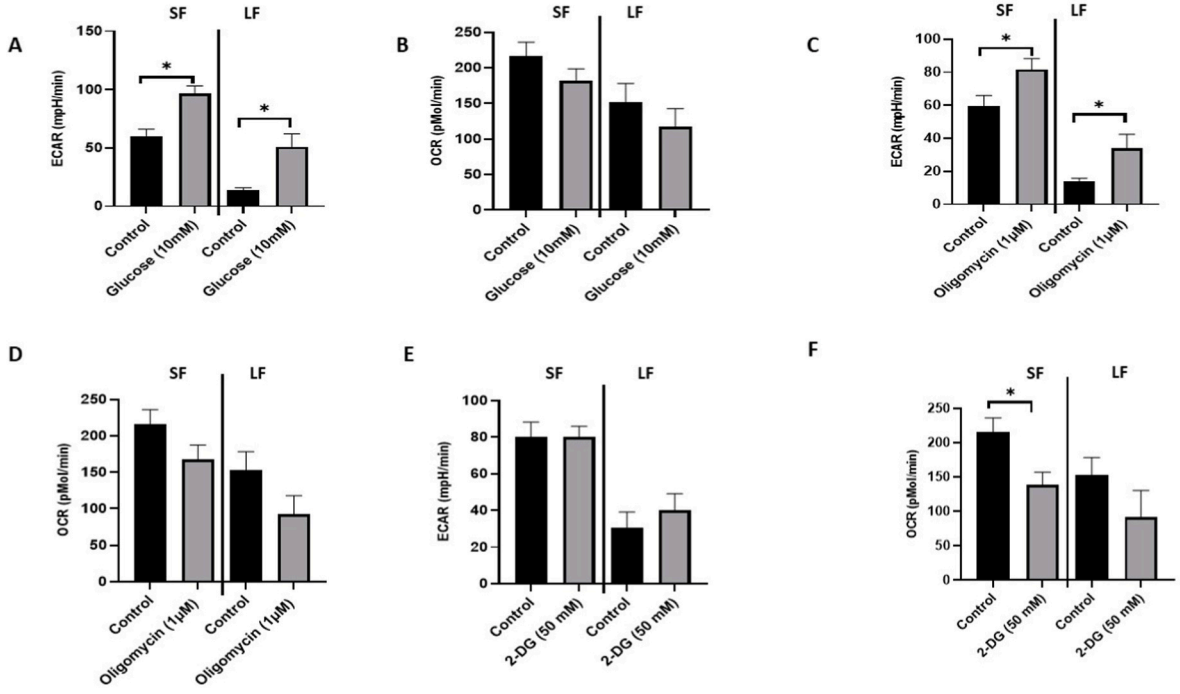

Fig. 2. ECAR and OCR of granulosa cells of bovine small (SF) and large (LF) antral follicles using a glycolysis stress test. For the glycolysis stress test, ECAR (**A**) and OCR (**B**) after stimulation with glucose ECAR (**C**) and OCR (**D**) after inhibition with Oligomycin, and ECAR (**E**) and OCR (**F**) after inhibition with 2-deoxy-D-glucose. Results represent n = 10 ovary pairs, run in triplicate, with the mean±SEM rate of the respective measurement shown. Asterisks denote a difference at $P < 0.05$.

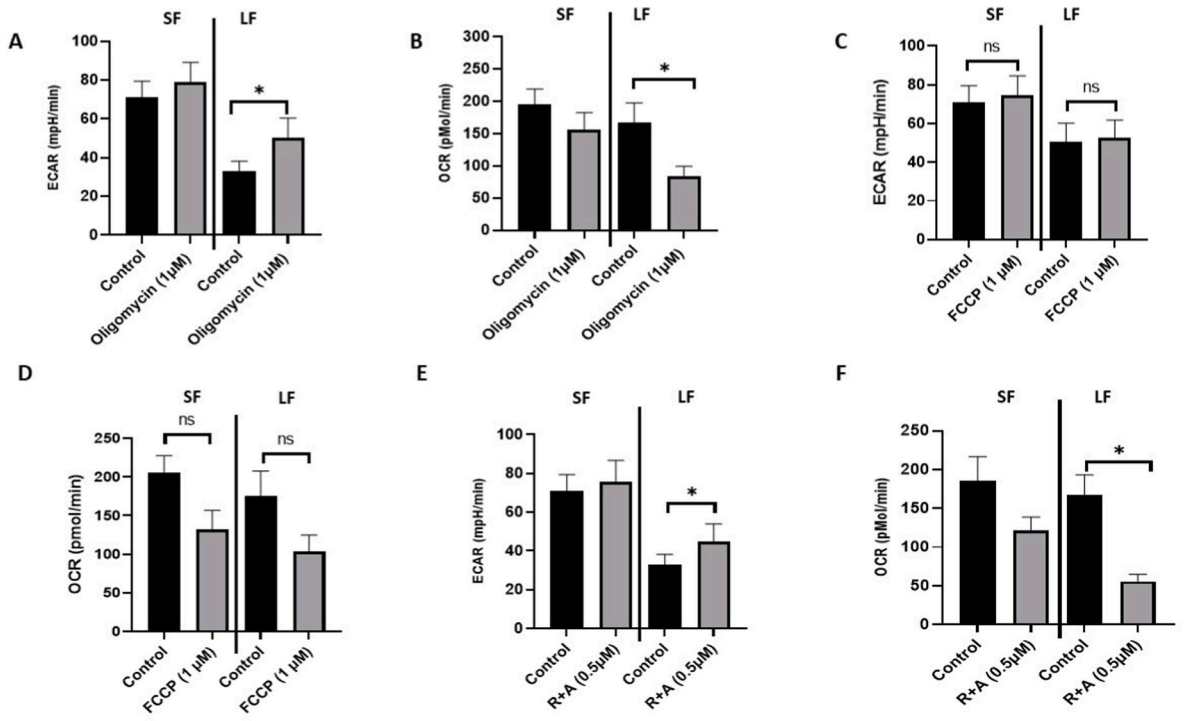

Fig. 3. ECAR and OCR of granulosa cells from bovine small and large antral follicles using a mitochondrial stress test. For the mitochondrial stress test, ECAR and OCR after inhibition with Oligomycin (**A** and **B**, respectively), uncoupling with FCCP (**C** and **D** respectively), or after inhibition with rotenone and antimycin A (R + A) (**E** and **F**, respectively). Results represent n = 10 ovary pairs, run in triplicate, with the mean±SEM of the respective measurement shown. Asterisks denote a difference at $P < 0.05$.

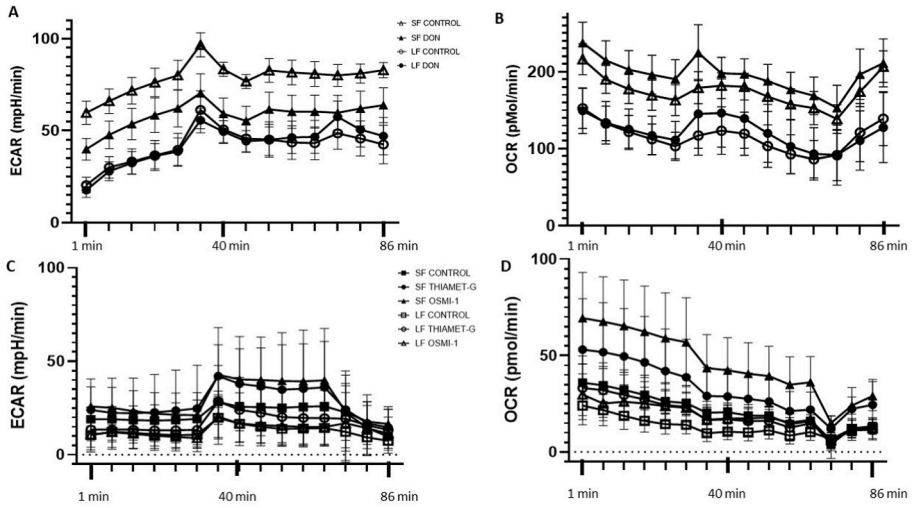

Fig. 4. Extracellular Acidification Rate (ECAR) and Oxygen Consumption Rate (OCR) of granulosa cells from bovine antral follicles following treatment with or without the glutamine fructose-6-phosphate aminotransferase (GFAT) inhibitor, DON, OGT inhibitor, OSMI-1, or OGA inhibitor, Thiamet-G. (**A**) Effect of 24 h exposure to DON (50 μM) on ECAR and (**B**) OCR of granulosa cells from small (SF; 3–5 mm) and large (LF; >8.5 mm) antral follicles. Effect of 24 hr exposure to OSMI-1 (50 μM) and Thiamet-G (2.5 μM) on (**C**) ECAR and (**D**) OCR of granulosa cells from small and large antral follicles. ECAR and OCR measurements were automatically recorded by the Wave software every 3 min, with treatment injections occurring every 18 min. Results represent n = 3 (C, D) or 10 (A, B) ovary pairs, run in triplicate, with the mean±SEM of the respective measurement shown.

3.5. Inhibition of O-GlcNAcylation impairs expression of glycolytic enzymes

Observing the similarity in expression of glycolytic enzymes between GCs of small and large antral follicles, we then examined the effect of manipulating O-GlcNAcylation on these same enzymes. As seen in Fig. 6, augmenting O-GlcNAcylation (via Thiamet-G) had no effect on any of these enzymes, regardless of follicle size (Fig. 6A and B; $P > 0.05$). Conversely, inhibition of O-GlcNAcylation (via OSMI-1) impaired the expression of hexokinase in GCs of small antral follicles only (Fig. 6A and B; $P < 0.05$) and inhibited the expression of phosphofructokinase, pyruvate kinase, and pyruvate dehydrogenase in GCs of both small and large antral follicles (Fig. 6A and B; $P < 0.05$). There was no effect of inhibition of O-GlcNAcylation on the expression of lactate dehydrogenase, regardless of follicle size (Fig. 6A and B; $P > 0.05$).

3.6. OGT inhibition via OSMI-1 does not affect OGT or OGA protein expression

As OSMI-1 impaired expression of glycolytic enzymes and has been shown to impair global O-GlcNAcylation in GCs (Maucieri and Townson, 2021), its effects on OGT and OGA expression were evaluated. No effects were observed for either OGT or OGA expression in GCs from small and large follicles (Fig. 7, $P > 0.05$).

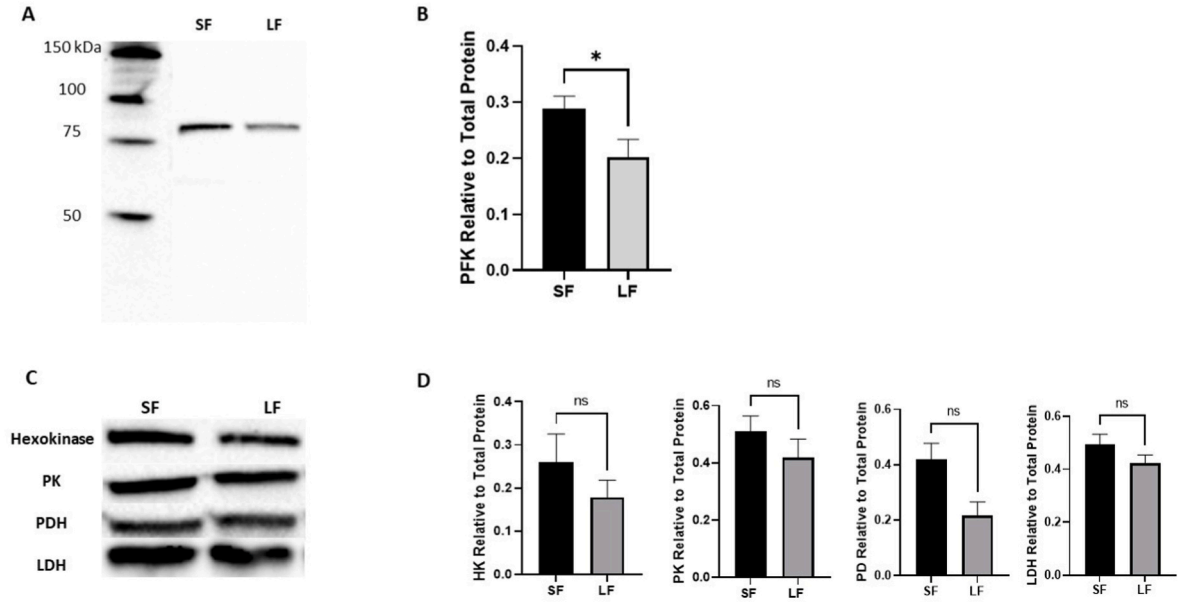

Fig. 5. Immunoblot and densitometric analyses of glycolytic enzyme expression in granulosa cells of bovine antral follicles. (**A**) Immunoblot of phosphofructokinase (PFK) expression (80 kDa) in granulosa cells of bovine small (SF; 3–5 mm) and large (LF; >8.5 mm) antral follicles. (**B**) Bar graph depicting densitometric analyses of PFK expression relative to total protein. (**C**) Immunoblots of hexokinase (HK, 102 kDa), pyruvate kinase (PK, 60 kDa), pyruvate dehydrogenase (PDH, 37 kDa), and lactate dehydrogenase (LDH, 37 kDa) expression in bovine granulsoa cells of small (SF; 3–5 mm) and large (LF; >8.5 mm) antral follicles. (**D**) Bar graphs depicting densitometric analyses of glycolytic enzyme expression relative to total protein. Results represent n = 4 ovary pairs, run in triplicate, with the mean±SEM of signal intensity shown. Asterisks denote differences between SF and LF at $P < 0.05$. ns = no significant difference, $P > 0.05$.

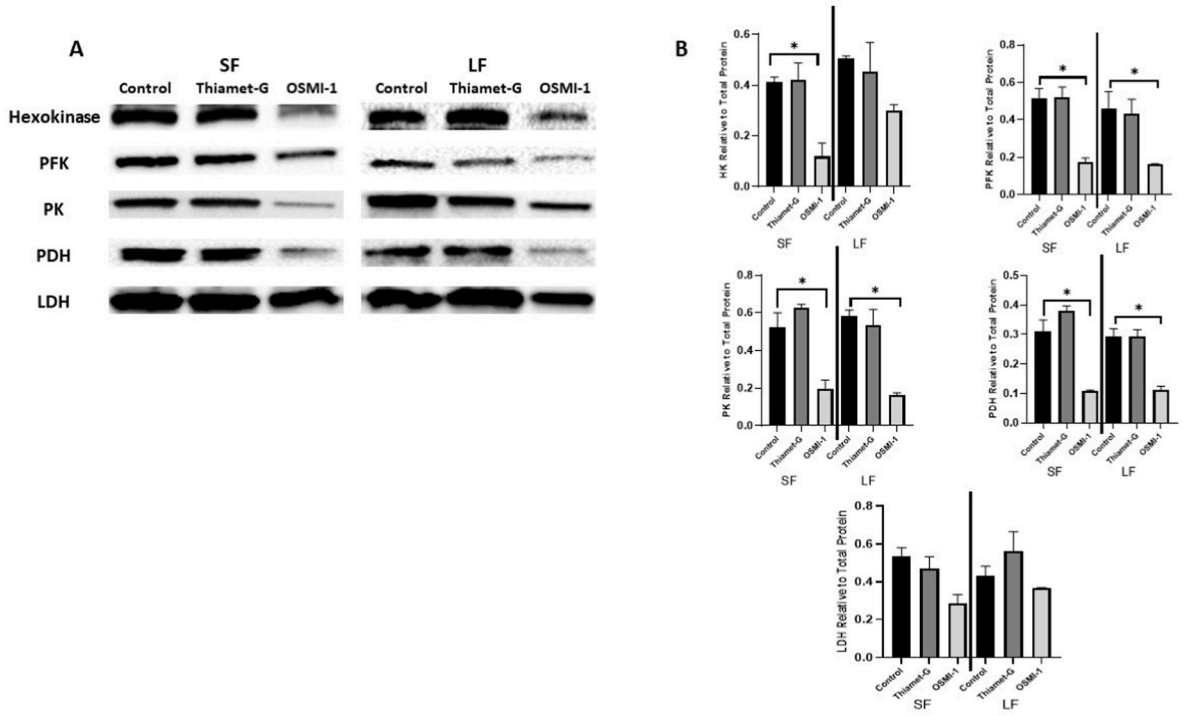

Fig. 6. Immunoblots and densitometric analyses of glycolytic enzyme expression under altered O-GlcNAc conditions. (**A**) Immunoblots of hexokinase (102 kDa), phosphofructokinase (PFK, 80 kDa), pyruvate kinase (PK, 60 kDa), pyruvate dehydrogenase (PDH, 37 kDa), and lactate dehydrogenase (LDH, 37 kDa) expression in bovine granulsoa cells of small (SF; 3–5 mm) and large (LF; >8.5 mm) antral follicles with or without exposure to Thiamet-G (2.5 μM) or OSMI-1 (50 μM). (**B**) Bar graphs depicting densitometric analyses of enzyme expression relative to total protein. Results represent n = 3 ovary pairs, run in triplicate, with the mean±SEM of signal intensity shown. Asterisks denote differences between treatments at $P < 0.05$.

4. Discussion

Glucose metabolism in preantral and early antral follicles is considered primarily glycolytic (Boland et al., 1993, 1994a; Harris et al., 2007; Leese and Lenton, 1990). Glycolytic metabolism diminishes the need for oxygen by granulosa and theca cells, allowing it to be conserved

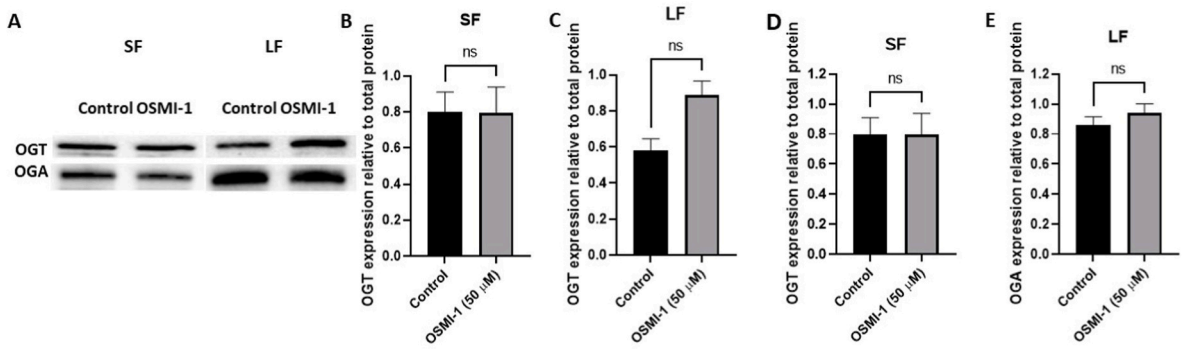

Fig. 7. Immunoblots and densitometric analyses of O-GlcNAc transferase (OGT) and O-GlcNAcase (OGA) expression under altered O-GlcNAc conditions. (**A**) OGT (110 kDa) and OGA (130 kDa) expression in bovine granulosa cells of small (SF; 3–5 mm) and large (LF; >8.5 mm) antral follicles without or with exposure to OSMI-1 (50 μM). (**B**, **C**, **D**, **E**) Bar graphs depicting densitometric analyses of enzyme expression relative to total protein. Results represent n = 4 ovary pairs, run in duplicate, with the mean±SEM of signal intensity shown.

for use by the oocyte exclusively (Biggers et al., 1967; Harris et al., 2007). Indeed, lactate is a major glycolytic product of follicular metabolism and this is supported by the observation that cultured GCs produce large quantities of lactate, even in the presence of oxygen (Billig et al., 1983; Boland et al., 1993; Leese and Barton, 1984). The current thinking is that glycolysis affords a rapid and efficient avenue for cells to convert glucose to ATP during rapid cell division. In the bovine ovary, small antral follicles consisting of highly proliferative GCs have less glucose, but greater lactate concentrations in the follicular fluid than large antral follicles in which GC proliferation has begun to wane (Maucieri and Townson, 2021). This suggests there may be a point during follicle maturation wherein GCs become less reliant on glycolysis for rapid growth, and transition to oxygen consuming pathways (i.e., oxidative phosphorylation) to support differentiation (e.g. luteinization) and steroidogenesis (e.g., estradiol production). Experiments in the current study are among the first, to our knowledge, to investigate these aspects of glycolytic and oxidative metabolism in GCs at the cellular level, using highly sensitive methods that can measure potential changes in metabolism in real time. Additionally, we evaluated the influence of the hexosamine biosynthesis pathway (HBP), and the novel process of O-GlcNAcylation, on glucose metabolism in GCs considering potential changes to glycolytic enzymes.

Consistent with previous work suggesting GCs transition from glycolytic to oxidative metabolism as follicles grow (Boland et al., 1993, 1994a, 1994b; Leroy et al., 2004b, 2008; Maucieri and Townson, 2021; Nandi et al., 2007; Orsi et al., 2005), we discovered direct evidence of this transition at the cellular level by measuring metabolism in cultured GCs using the Seahorse XFe96 analyzer. This machine detects extracellular proton secretion and oxygen consumption as indices of glycolysis and oxidative phosphorylation, respectively, in real time. Using an established glycolytic stress test, we determined that cultures of GCs from small antral follicles were acutely sensitive to glucose availability and relied upon glycolysis (with or without oxidative phosphorylation) to provide cellular energy. The increase in ECAR, without an accompanying effect on OCR, following an influx of glucose is indicative of this action (Fig. 2 A and B). Additionally, inhibiting oxidative phosphorylation via oligomycin had no effect on OCR, but again increased ECAR (Fig. 2 C and D), inferring that GCs from small antral follicles do not rely on oxidative phosphorylation as part of their metabolism. Conversely, cultures of GCs from large antral follicles ostensibly have the capacity to utilize a variety of energy substrates (i.e., glutamine, fatty acids, etc.), and readily metabolize them via oxidative phosphorylation. This was evident during the portion of the glycolytic stress test in which 2-deoxy-D-glucose (2-DG, a non-metabolizable form of glucose) was introduced. Briefly, oxidative phosphorylation (as measured by OCR) continued unimpeded, but only in GCs from large antral follicles (Fig. 2F). The decline in OCR in response to 2-DG in GCs from small antral follicles (Fig. 2F) suggests these cells rely upon glucose processed directly through glycolysis to provide cellular energy. In similar work conducted by Shiratsuki and coworkers, cultured bovine GCs in the presence of low oxygen levels (5%) exhibited upregulated glycolysis and increased cellular proliferation (Shiratsuki et al., 2016). Such dependence upon glycolysis versus oxygen consumption is likely cell type specific. This thinking is supported by studies from others who found that the OCR of cancer cells, for instance, remains unaffected by treatment with 2-DG (Wu et al., 2007). In contrast, neuronal cells exhibit a remarkable decline in OCR when exposed to 2-DG (Dodson et al., 2022). Collectively, these observations support the concept that glycolysis shifts toward oxidative phosphorylation as GCs mature within growing antral follicles. They also complement the results of previous studies in which metabolic endpoints were measured primarily using whole follicle cultures and mouse models (Boland et al., 1993, 1994a, 1994b; Gook et al., 2014).

Conceptually, the transition of glucose metabolism as GCs mature and further differentiate in growing antral follicles is becoming clearer, but the rationale as to why this transition occurs is less understandable. Perhaps GCs extensively metabolize glucose glycolytically during early follicle development to support the oocyte that, alone, executes glycolysis inefficiently (Sugiura et al., 2005). Unlike oocytes, GCs produce large quantities of pyruvate and lactate, which in turn serve as ideal metabolic substrates for oocytes (Donahue and Stern, 1968; Leese and Barton, 1985). The metabolic transition in GCs may also be controlled by the demands of the oocyte, wherein direct (Eppig, 1979, 1991) and indirect communication (Sugiura et al., 2005) occurs. In this manner the advancement of follicular growth might be intrinsically regulated, influenced by granulosa cell-oocyte communication as well as the transition in glucose metabolism. Oxidative metabolism favors the capacity of GCs of large antral follicles to produce increased amounts of steroid. Gonadotropins stimulate oxygen uptake in mitochondria of ovarian cells, and this effect accompanies an increase in steroidogenesis (Dimino et al., 1980). Regardless of whether or not the transition in GCs occurs to support the oocyte, is controlled by the oocyte, and/or simply reflects greater capacity of the GCs to differentiate and produce steroid, a similar pivot in glucose metabolism also occurs during *in vitro* development of murine oocytes and *in vitro* derived bovine embryos (Harris et al., 2009; Thompson et al., 1996).

In this study, although inhibition of the HBP (via DON) had no adverse effect on glucose metabolism by GCs (i.e., ECAR and OCR), the downstream disruption of O-GlcNAcylation directly (via OSMI-1) provided evidence that GCs from small antral follicles remain reliant on glucose as a primary substrate. An absence of glucose channeled through the HBP to facilitate O-GlcNAcylation had no effect on metabolism, but it did impair the expression of enzymes involved with glycolysis. In other studies, disruption of O-GlcNAc cycling also reduces

mitochondrial membrane potential and ATP production (Wang et al., 2022). In the current work, direct inhibition of O-GlcNAcylation (via OSMI-1) impaired the expression of phosphofructokinase, pyruvate kinase, and pyruvate dehydrogenase (Fig. 6) in GCs of both small and large antral follicles. This outcome is consistent with the Wang and coworkers study in which GCs were treated with BADGP, another OGT inhibitor, that inhibited the activity of pyruvate kinase (Wang et al., 2022). Hexokinase expression, a key enzyme for both glucose utilization (via the HBP) and metabolism (via glycolysis), was impaired only in GCs of small antral follicles (Fig. 6). Thus, a connection likely exists between O-GlcNAcylation and the regulation of glycolysis, particularly in GCs of small antral follicles, but it is unclear why inhibition of the HBP and O-GlcNAcylation failed to impact glucose metabolism in the current study. Perhaps stimulating steroidogenesis and stressing metabolic capacity of the GCs of small follicles with gonadotropin (i.e., FSH) and/or growth factor (IGF-1) driven conditions is needed. LH and FSH reportedly increase glucose uptake and glycolysis in granulosa cells (Billig et al., 1983; Boland et al., 1993; Hillier et al., 1985) and IGF-1 mobilizes GLUT 4 (Dupont and Scaramuzzi, 2016). In any event, this area offers fertile ground for future investigation, and at least one study has determined that the glycolytic enzymes, phosphofructokinase, pyruvate kinase, and lactate dehydrogenase, are all modified by O-GlcNAcylation (Wang et al., 2017). Here we provide evidence that some of these same enzymes might be modified by O-GlcNAc and regulated by the degree of O-GlcNAcylation in bovine GCs.

5. Conclusion

In conclusion, granulosa cells (GCs) from bovine small antral follicles exhibit greater overall glucose metabolism than GCs of large antral follicles and are more reliant on aerobic glycolysis than oxidative phosphorylation. During folliculogenesis, GCs of antral follicles apparently undergo a transition in metabolism primarily from aerobic glycolysis to oxidative phosphorylation as the follicle grows. The reasons for this require further investigation, but it is likely that the transition facilitates the rapid growth and maturation of the follicle. Although inhibition of the hexosamine biosynthesis pathway in this study failed to adversely affect GC metabolism, it appears there are effects downstream (via direct inhibition of O-GlcNAcylation) in which expression of glycolytic enzymes is impaired. Thus, a relationship between O-GlcNAcylation and glycolytic metabolism in bovine GCs is supported (Fig. 8). Future work will help determine whether direct O-GlcNAcylation of glycolytic enzymes impacts the metabolism, function, and fate of the GCs.

Grant support

This work was supported by USDA Hatch Funds, USDA Multistate Project NE-1727 (DHT), and USDA-AFRI NIFA Grant #2020-6701631018.

CRediT authorship contribution statement

Abigail M. Maucieri: Conceptualization, the study, experimental

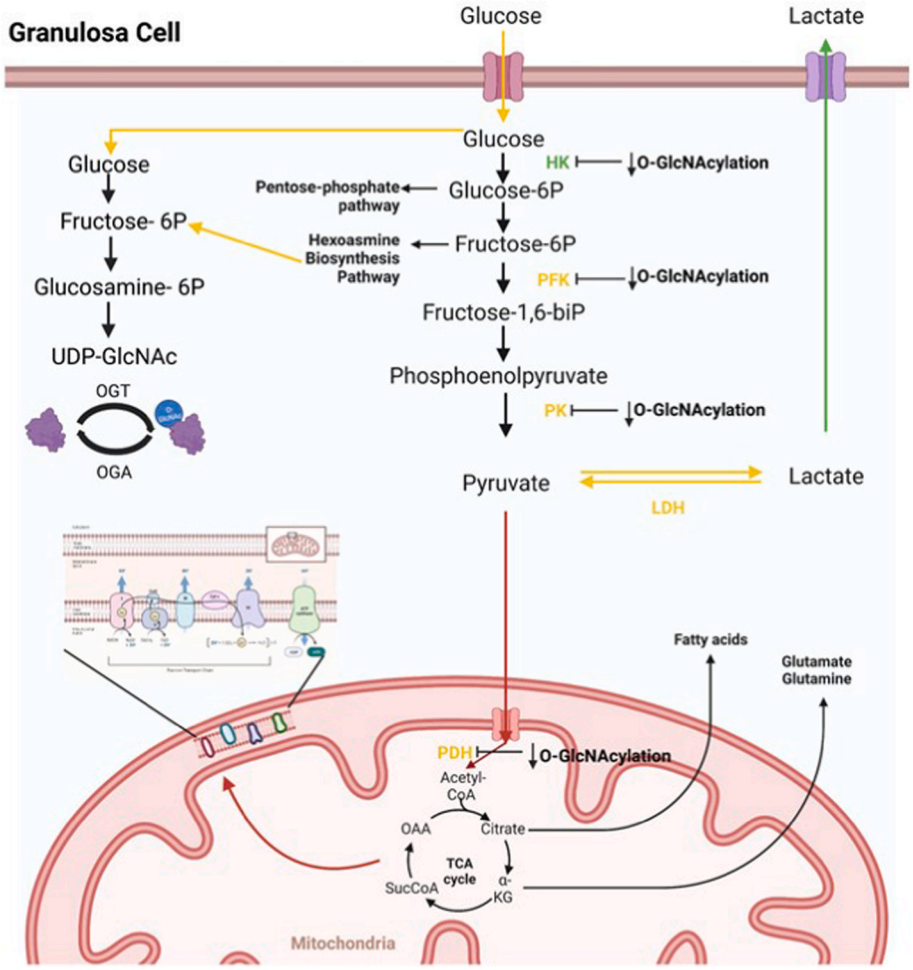

Fig. 8. A schematic summarizing the impact of O-GlcNAcylation and a proposed model of glucose utilization in granulosa cells (GCs) of bovine antral follicles. Colored arrows and text denote pathways and effects of O-GlcNAcylation on glycolytic enzymes, respectively, corresponding to GCs of small antral follicles (GREEN), large antral follicles (RED), or both types of antral follicles (YELLOW). Glucose uptake by both types of follicles is processed similarly through the hexosamine biosynthesis pathway for O-GlcNAcylation (upper LEFT) and the glycolytic pathway (MIDDLE). However, whereas GCs of small follicles metabolize glucose glycolytically (resulting in lactate production), GCs of large follicles further process glucose through oxidative phosphorylation in the mitochondria. Notably, disruption of O-GlcNAcylation affects specific glycolytic enzymes, in a follicle size dependent manner. Glucose 6-phosphate (Glucose-6P), fructose 6-phosphate (Fructose-6P), fructose 1–6, bisphosphate (Fructose-1-6, biP), Glucosamine 6-phosphate (Glucosamine-6P), O-GlcNAc transferase (OGT), O-GlcNAcase (OGA) hexokinase (HK), phosphofructokinase (PFK) pyruvate kinase (PK), lactate dehydrogenase (LDH), pyruvate dehydrogenase (PDH). Created with biorender.com.

design, and wrote and revised the manuscript, performed the experiments, Data curation, and conducted the statistical, Formal analysis. **David H. Townson:** Conceptualization, the study, experimental design, and wrote and revised the manuscript, acquired funding and provided the resources needed to complete the experiments and manuscript. 17.

Declarations of competing interest

None.

Data availability

Data will be made available on request.

References

Allen, W.R., Nilsen-Hamilton, M., Hamilton, R.T., 1981. Insulin and growth factors stimulate rapid posttranslational changes in glucose transport in ovarian granulosa cells. J. Cell. Physiol. 108, 15–24. https://doi.org/10.1002/jcp.1041080104.

Armstrong, D.T., Kilpatrick, R., Greep, R.O., 1963. In vitro and in vivo stimulation of glycolysis in prepubertal rat ovary by luteinizing hormone. Endocrinology 73, 165–169. https://doi.org/10.1210/endo-73-2-165.

Biggers, J.D., Whittingham, D.G., Donahue, R.P., 1967. The pattern of energy metabolism in the mouse oöcyte and zygote. Proc. Natl. Acad. Sci. USA 58, 560–567. https://doi.org/10.1073/pnas.58.2.560.

Billig, H., Hedin, L., Magnusson, C., 1983. Gonadotrophins stimulate lactate production by rat cumulus and granulosa cells. Acta Endocrinol. 103, 562–566. https://doi.org/10.1530/acta.0.1030562.

Boland, N., Humpherson, P., Leese, H., Gosden, R., 1994. The effects of glucose metabolism on murine follicle development and steroidogensis in vitro. Hum. Reprod. 9, 617–623.

Boland, N.I., Humpherson, P.G., Leese, H.J., Gosden, R.G., 1994a. Characterization of follicular energy metabolism. Hum. Reprod. 9, 604–609. https://doi.org/10.1093/oxfordjournals.humrep.a138557.

Boland, N.I., Humpherson, P.G., Leese, H.J., Gosden, R.G., 1994b. The effect of glucose metabolism on murine follicle development and steroidogenesis in vitro. Hum. Reprod. 9, 617–623. https://doi.org/10.1093/oxfordjournals.humrep.a138559.

Boland, N.I., Humpherson, P.G., Leese, H.J., Gosden, R.G., 1993. Pattern of lactate production and steroidogenesis during growth and maturation of mouse ovarian follicles in Vitro1. Biol. Reprod. 48, 798–806. https://doi.org/10.1095/biolreprod48.4.798.

Bond, M.R., Hanover, J.A., 2015. A little sugar goes a long way: the cell biology of O-GlcNAc. J. Cell Biol. 208, 869–880. https://doi.org/10.1083/jcb.201501101.

Buse, M.G., Robinson, K.A., Marshall, B.A., Hresko, R.C., Mueckler, M.M., 2002. Enhanced *O* -GlcNAc protein modification is associated with insulin resistance in GLUT1-overexpressing muscles. Am. J. Physiol. Metab. 283, E241–E250. https://doi.org/10.1152/ajpendo.00060.2002.

Campbell, B., Onions, V., Kendall, N., Guo, L., Scaramuzzi, R., 2010. The effect of monosaccharide sugars and pyruvate on the differentiation and metabolism of sheep granulosa cells in vitro. Reproduction 140, 541–550. https://doi.org/10.1530/REP-10-0146.

Copeland, R.J., Bullen, J.W., Hart, G.W., 2008. Cross-talk between GlcNAcylation and phosphorylation: roles in insulin resistance and glucose toxicity. Am. J. Physiol. Endocrinol. Metab. https://doi.org/10.1152/ajpendo.90281.2008.

Costermans, N.G.J., Keijer, J., van Schothorst, E.M., Kemp, B., Keshtkar, S., Bunschoten, A., Soede, N.M., Teerds, K.J., 2019. In ovaries with high or low variation in follicle size, granulosa cells of antral follicles exhibit distinct size-related processes. Mol. Hum. Reprod. 25, 614–624. https://doi.org/10.1093/MOLEHR/GAZ042.

De Koster, J.D., Opsomer, G., 2013. Insulin resistance in dairy cows. Vet. Clin. North Am. - Food Anim. Pract. 29, 299–322. https://doi.org/10.1016/j.cvfa.2013.04.002.

Dehennaut, V., Slomianny, M.C., Page, A., Vercoutter-Edouart, A.S., Jessus, C., Michalski, J.C., Vilain, J.P., Bodart, J.F., Lefebvre, T., 2008. Identification of structural and functional O-linked N-acetylglucosamine-bearing proteins in Xenopus laevis oocyte. Mol. Cell. Proteomics 7, 2229–2245. https://doi.org/10.1074/mcp.M700494-MCP200.

Dimino, M.J., Chavis, T.R., Dowing, J.R., 1980. A relationship between adenosine 5′-triphosphate and pregnenolone syntheses by ovarian mitochondria as demonstrated with aminoglutethimide. Endocrinology 106, 1528–1531. https://doi.org/10.1210/endo-106-5-1528.

Dodson, M., Benavides, G.A., Darley-Usmar, V., Zhang, J., 2022. Differential effects of 2-deoxyglucose and glucose deprivation on 4-hydroxynonenal dependent mitochondrial dysfunction in primary neurons. Front. Aging 3. https://doi.org/10.3389/fragi.2022.812810.

Donahue, R.P., Stern, S., 1968. Follicular cell support of oocyte maturation: production of pyruvate in vitro. Reproduction 17, 395–398. https://doi.org/10.1530/jrf.0.0170395.

Dupont, J., Scaramuzzi, R.J., 2016. Insulin signalling and glucose transport in the ovary and ovarian function during the ovarian cycle. Biochem. J. https://doi.org/10.1042/BCJ20160124.

Eppig, J.J., 1991. Intercommunication between mammalian oocytes and companion somatic cells. Bioessays 13, 569–574. https://doi.org/10.1002/BIES.950131105.

Eppig, J.J., 1979. A comparison between oocyte growth in coculture with granulosa cells and oocuytes with granulosa-cell junctional contact maintained in vitro. J. Exp. Zool. 209, 345–353. https://doi.org/10.1002/jez.1402090216.

Flint, A.P.F., Denton, R.M., 1969. Glucose Metabolism in the Superovulated Rat Ovary in vitro. Effects of luteinizing hormone and the role of glucose metabolism in steroidogenesis. Biochem. J. https://doi.org/10.1042/bj1120243.

Gook, D.A., Edgar, D.H., Lewis, K., Sheedy, J.R., Gardner, D.K., 2014. Impact of oxygen concentration on adult murine pre-antral follicle development in vitro and the corresponding metabolic profile. Mol. Hum. Reprod. 20, 31–41. https://doi.org/10.1093/MOLEHR/GAT062.

Hardivillé, S., Hart, G.W., 2014. Nutrient Regulation of Signaling, Transcription, and Cell Physiology by O- GlcNAcylation. Cell Metab. https://doi.org/10.1016/j.cmet.2014.07.014.

Harris, S.E., Adriaens, I., Leese, H.J., Gosden, R.G., Picton, H.M., 2007. Carbohydrate metabolism by murine ovarian follicles and oocytes grown in vitro. Reproduction 134, 415–424. https://doi.org/10.1530/REP-07-0061.

Harris, S.E., Leese, H.J., Gosden, R.G., Picton, H.M., 2009. Pyruvate and oxygen consumption throughout the growth and development of murine oocytes. Mol. Reprod. Dev. 76, 231–238. https://doi.org/10.1002/mrd.20945.

Hart, G.W., Akimoto, Y., 2009. The O-GlcNAc modification. In: Essentials of Glycobiology. Cold Spring Harbor Laboratory Press.

Hillier, S.G., Purohit, A., Reichert, L.E., 1985. Control of granulosa cell lactate production by follicle-stimulating hormone and androgen. Endocrinology 116, 1163–1167. https://doi.org/10.1210/endo-116-3-1163.

Ireland, J.J., Murphee, R.L., Coulson, P.B., 1980. Accuracy of predicting stages of bovine estrous cycle by gross appearance of the corpus luteum. J. Dairy Sci. 63, 155–160. https://doi.org/10.3168/jds.S0022-0302(80)82901-8.

Kim, E., Seok, H.H., Lee, D.-R., Yoon, T.-K., Lee, W.-S., Lee, K.-A., 2010. Expression of glucose transporters (GLUTS) in granulosa cells according to insulin resistance and metabolic syndrome in PCOS pateints. Fertil. Steril. 94, S192. https://doi.org/10.1016/j.fertnstert.2010.07.748.

Leese, H.J., Barton, A.M., 1985. Production of pyruvate by isolated mouse cumulus cells. J. Exp. Zool. 234, 231–236. https://doi.org/10.1002/jez.1402340208.

Leese, H.J., Barton, A.M., 1984. Pyruvate and glucose uptake by mouse ova and preimplantation embryos. Reproduction 72, 9–13. https://doi.org/10.1530/jrf.0.0720009.

Leese, H.J., Lenton, E.A., 1990. Glucose and lactate in human follicular fluid: concentrations and interrelationships. Hum. Reprod. 5, 915–919. https://doi.org/10.1093/oxfordjournals.humrep.a137219.

Lefebvre, T., Dehennaut, V., Guinez, C., Olivier, S., Drougat, L., Mir, A.M., Mortuaire, M., Vercoutter-Edouart, A.S., Michalski, J.C., 2010. Dysregulation of the nutrient/stress sensor O-GlcNAcylation is involved in the etiology of cardiovascular disorders, type-2 diabetes and Alzheimer's disease. Biochim. Biophys. Acta, Gen. Subj. https://doi.org/10.1016/j.bbagen.2009.08.008.

Leroy, J.L.M.R., Van Soom, A., Opsomer, G., Bols, P.E.J., 2008. The consequences of metabolic changes in high-yielding dairy cows on oocyte and embryo quality. Animal 2, 1120–1127. https://doi.org/10.1017/s1751731108002383.

Leroy, J.L.M.R., Vanholder, T., Delanghe, J.R., Opsomer, G., Van Soom, A., Bols, P.E.J., De Kruif, A., 2004a. Metabolite and ionic composition of follicular fluid from different-sized follicles and their relationship to serum concentrations in dairy cows. Anim. Reprod. Sci. 80, 201–211. https://doi.org/10.1016/S0378-4320(03)00173-8.

Leroy, J.L.M.R., Vanholder, T., Delanghe, J.R., Opsomer, G., Van Soom, A., Bols, P.E.J., Dewulf, J., De Kruif, A., 2004b. Metabolic changes in follicular fluid of the dominant follicle in high-yielding dairy cows early post partum. Theriogenology 62, 1131–1143. https://doi.org/10.1016/j.theriogenology.2003.12.017.

Lucy, M.C., 2016a. The role of glucose in dairy cattle reproduction. WCDS Adv. Dairy Technol. 28, 161–173.

Lucy, M.C., 2016b. Mechanisms linking postpartum metabolism and reproduction. WCDS Adv. Dairy Technol. 28, 259–269.

Ma, J., Hart, G.W., 2013. Protein O-GlcNAcylation in diabetes and diabetic complications. Expert Rev. Proteomics. https://doi.org/10.1586/14789450.2013.820536.

Maucieri, A.M., Townson, D.H., 2021. Evidence and manipulation of O-GlcNAcylation in granulosa cells of bovine antral follicles. Biol. Reprod. 104, 914–923. https://doi.org/10.1093/biolre/ioab013.

Nandi, S., Girish Kumar, V., Manjunatha, B.M., Ramesh, H.S., Gupta, P.S.P., 2008. Follicular fluid concentrations of glucose, lactate and pyruvate in buffalo and sheep, and their effects on cultured oocytes, granulosa and cumulus cells. Theriogenology 69, 186–196. https://doi.org/10.1016/j.theriogenology.2007.08.036.

Nandi, S., Kumar, V.G., Manjunatha, B.M., Gupta, P.S.P., 2007. Biochemical composition of ovine follicular fluid in relation to follicle size. Dev. Growth Differ. 49, 61–66. https://doi.org/10.1111/j.1440-169X.2007.00901.x.

Orsi, N.M., Gopichandran, N., Leese, H.J., Picton, H.M., Harris, S.E., 2005. Fluctuations in bovine ovarian follicular fluid composition throughout the oestrous cycle. Reproduction 129, 219–228. https://doi.org/10.1530/rep.1.00460.

Ortiz-Meoz, R.F., Jiang, J., Lazarus, M.B., Orman, M., Janetzko, J., Fan, C., Duveau, D.Y., Tan, Z.W., Thomas, C.J., Walker, S., 2015. A small molecule that inhibits OGT activity in cells. ACS Chem. Biol. 10, 1392–1397. https://doi.org/10.1021/acschembio.5b00004.

Shiratsuki, S., Hara, T., Munakata, Y., Shirasuna, K., Kuwayama, T., Iwata, H., 2016. Low oxygen level increases proliferation and metabolic changes in bovine granulosa cells. Mol. Cell. Endocrinol. 437, 75–85. https://doi.org/10.1016/j.mce.2016.08.010.

Sugiura, K., Pendola, F.L., Eppig, J.J., 2005. Oocyte control of metabolic cooperativity between oocytes and companion granulosa cells: energy metabolism. Dev. Biol. 279, 20–30. https://doi.org/10.1016/j.ydbio.2004.11.027.

Sun, H., Chen, L., Cao, S., Liang, Y., Xu, Y., 2019. Warburg effects in cancer and normal proliferating cells: two tales of the same name. Genomics. Proteomics Bioinformatics 17, 273–286. https://doi.org/10.1016/j.gpb.2018.12.006.

Tekade, R.K., Sun, X., 2017. The Warburg effect and glucose-derived cancer theranostics. Drug Discov. Today. https://doi.org/10.1016/j.drudis.2017.08.003.

Thompson, J.G., Partridge, R.J., Houghton, F.D., Cox, C.I., Leese, H.J., 1996. Oxygen uptake and carbohydrate metabolism by in vitro derived bovine embryos. Reproduction 106, 299–306. https://doi.org/10.1530/jrf.0.1060299.

Van Blerkom, J., Antczak, M., Schrader, R., 1997. The developmental potential of the human oocyte is related to the dissolved oxygen content of follicular fluid: association with vascular endothelial growth factor levels and perifollicular blood flow characteristics. Hum. Reprod. 12, 1047–1055. https://doi.org/10.1093/humrep/12.5.1047.

Walter, L.A., Lin, Y.H., Halbrook, C.J., Chuh, K.N., He, L., Pedowitz, N.J., Batt, A.R., Brennan, C.K., Stiles, B.L., Lyssiotis, C.A., Pratt, M.R., 2020. Inhibiting the hexosamine biosynthetic pathway lowers O-GlcNAcylation levels and sensitizes cancer to environmental stress. Biochemistry 59, 3169–3179. https://doi.org/10.1021/acs.biochem.9b00560.

Wang, T.-F., Feng, Z.-Q., Sun, Y.-W., Zhao, S.-J., Zou, H.-Y., Hao, H.-S., Du, W.-H., Zhao, X.-M., Zhu, H.-B., Pang, Y.-W., 2022. Disruption of O-GlcNAcylation homeostasis induced ovarian granulosa cell injury in bovine. Int. J. Mol. Sci. 23, 7815. https://doi.org/10.3390/ijms23147815.

Wang, Y., Liu, J., Jin, X., Zhang, D., Li, D., Hao, F., Feng, Y., Gu, S., Meng, F., Tian, M., Zheng, Y., Xin, L., Zhang, X., Han, X., Aravind, L., Wei, M., 2017. O-GlcNAcylation destabilizes the active tetrameric PKM2 to promote the Warburg effect. Proc. Natl. Acad. Sci. U. S. A 114, 13732–13737. https://doi.org/10.1073/pnas.1704145115.

Wani, W.Y., Ouyang, X., Benavides, G.A., Redmann, M., Cofield, S.S., Shacka, J.J., Chatham, J.C., Darley-Usmar, V., Zhang, J., 2017. O-GlcNAc regulation of autophagy and α-synuclein homeostasis; Implications for Parkinson's disease. Mol. Brain 10. https://doi.org/10.1186/s13041-017-0311-1.

Warburg, O., 1925. The metabolism of carcinoma cells 1. J. Cancer Res. 9, 148–163. https://doi.org/10.1158/jcr.1925.148.

Wu, M., Neilson, A., Swift, A.L., Moran, R., Tamagnine, J., Parslow, D., Armistead, S., Lemire, K., Orrell, J., Teich, J., Chomicz, S., Ferrick, D.A., 2007. Multiparameter metabolic analysis reveals a close link between attenuated mitochondrial bioenergetic function and enhanced glycolysis dependency in human tumor cells. Am. J. Physiol. Cell Physiol. 292, 125–136. https://doi.org/10.1152/AJPCELL.00247.2006/ASSET/IMAGES/LARGE/ZH00010750750009.JPEG.

Yuzwa, S.A., Macauley, M.S., Heinonen, J.E., Shan, X., Dennis, R.J., He, Y., Whitworth, G.E., Stubbs, K.A., McEachern, E.J., Davies, G.J., Vocadlo, D.J., 2008. A potent mechanism-inspired O-GlcNAcase inhibitor that blocks phosphorylation of tau in vivo. Nat. Chem. Biol. 4, 483–490. https://doi.org/10.1038/nchembio.96.

Zhang, J., Zhang, Q., 2019. Using Seahorse Machine to Measure OCR and ECAR in Cancer Cells, pp. 353–363. https://doi.org/10.1007/978-1-4939-9027-6_18.

Zhou, L.T., Romar, R., Pavone, M.E., Soriano-Úbeda, C., Zhang, J., Slawson, C., Duncan, F.E., 2019. Disruption of *O* -GlcNAc homeostasis during mammalian oocyte meiotic maturation impacts fertilization. Mol. Reprod. Dev. 86, 543–557. https://doi.org/10.1002/mrd.23131.